Chinese Journal of
POLYMER SCIENCE

RESEARCH ARTICLE

https://doi.org/10.1007/s10118-026-3684-8
Chinese J. Polym. Sci. **2026**, *44*, 1738–1748

Strong and Tough High-water Content Double-network Hydrogels

Shu-Xing Yin[a,†], Guo-Jun Che[b,†], Cheng Qian[a], Meng Yu[b], Can Zhou[b], Sheng-Wen Kong[b*], Chuang-Qi Zhao[a,b*], and Lei Jiang[a,b]

[a] *State Key Laboratory of Bioinspired Interfacial Materials Science, School of Chemistry and Materials Science, University of Science and Technology of China, Hefei 230026, China*
[b] *State Key Laboratory of Bioinspired Interfacial Materials Science, Suzhou Institute for Advanced Research, University of Science and Technology of China, Suzhou 215123, China*

Electronic Supplementary Information

Abstract Hydrogels have been widely used in tissue engineering and biomedical applications owing to their high water content and tunable functionality. Nevertheless, high water content and loosely cross-linked networks restrict the mechanical properties of hydrogels and their practical applications. Herein, we present a facile approach for designing strong and tough bacterial cellulose/poly(vinyl alcohol) (BC/PVA) double-network hydrogels involving immersing BC into PVA solutions and then freezing-thawing. The PVA chains encapsulate the BC nanofibers through hydrogen bonding interactions and chain entanglement, infiltrate the fibrous network, and thereby enhance the densification of the BC/PVA hydrogel. Concurrently, repetitive freeze-thaw cycles facilitate the regulation of PVA chain conformation and promote PVA crystallization, which increases the rigidity of the PVA segments. The resulted hydrogel demonstrates an exceptional tensile strength of (2.13±0.03) MPa, a remarkable toughness of (1.15±0.03) MJ·m^{-3}, and a high water content of up to 95%. Furthermore, the double-network hydrogels exhibit excellent biocompatibility. This study offers a practical strategy for the design of robust and tough hydrogels with potential utility in biomedical applications.

Keywords Strong and tough hydrogels; Double-network; Hydrogen bond; Network densification

Citation: Yin, S. X.; Che, G. J.; Qian, C.; Yu, M.; Zhou, C.; Kong, S. W.; Zhao, C. Q.; Jiang, L. Strong and tough high-water content double-network hydrogels. *Chinese J. Polym. Sci.* **2026**, *44*, 1738–1748.

INTRODUCTION

Hydrogels are 3D crosslinked polymeric networks with high water content flexibility.[1,2] Owing to their good biocompatibility[3–5] and tunable functionality[6], they are regarded as promising candidates for biomedical and bioelectrical applications.[7–10] Nevertheless, hydrogels demonstrate limited tensile strength and toughness attributable to their loosely cross-linked networks arising from their high water content, which severely restricts their applications.[11–15] Various strategies have been explored to fabricate hydrogels with high mechanical performance, such as designing dual networks,[16–18] constructing supramolecular or ordered architectures,[19] forming crystalline domains and phase separation,[20–29] and incorporating chain entanglements,[30–32] dynamic crosslinking sites, and nanofillers.[33,34] While the aforementioned strategies enable the fabrication of strong and tough hydrogels, they fail to simultaneously ensure high water content.[35]

Bacterial cellulose (BC) hydrogels consist of an interconnected network of nanofibers with water content of up to 99%.[36,37] The abundance of hydroxyl groups enable BC to form dimensionally stable hydrogel structures with exceptional structural integrity.[38] Furthermore, the high aspect ratios and elevated Young's modulus of the nanofibers within the network are beneficial for improving mechanical properties of BC-based hydrogels.[39,40] However, owing to their high crystallinity and rigid molecular chains, BC hydrogels generally exhibit limited deformability, which restricts their practical application. To address this limitation and fully exploit the potential of BC hydrogels, researchers have developed double-network (DN) hydrogels, in which BC is integrated with a second, more ductile polymer network.[38,41] For instance, incorporating natural polymers such as gelatin and sodium alginate into the BC matrix can significantly enhance the compressive fracture strength and elastic modulus, reaching levels comparable to those of articular cartilage.[38] However, although these combinations improve toughness, they often rely on specific cross-linking agents. Therefore, the exploration of polymers that offer both superior toughness and strong interfacial compatibility with BC remains a priority.

Poly(vinyl alcohol) (PVA) is a promising candidate for BC-based composite hydrogels because of its abundant hydroxyl groups that facilitate strong interfacial interactions with BC nanofibers *via* extensive hydrogen bonding.[41] Furthermore, PVA chains can be adjusted to form crystalline domains,

* Corresponding authors, E-mail: kongsw@ustc.edu.cn (S.W.K.)
E-mail: zhaochuangqi@ustc.edu.cn (C.Q.Z.)
† These authors contributed equally to this work.
Special Topic: Functional Gels
Received February 27, 2026; Accepted March 26, 2026; Published online May 20, 2026

thereby enhancing the mechanical properties of hydrogels.[19,20] While numerous studies have reported the mechanical performance of such composites, there is a lack of research on the underlying microstructural evolution and its contribution to mechanical reinforcement.

Here, we report a versatile freeze-thawing strategy to construct BC/PVA composite hydrogel with highly tailored properties. By changing the number of freeze-thaw cycles to control PVA crystallinity, the mechanical performance, such as modulus and strength, of hydrogels can be reasonably regulated. Microstructural analysis indicated that the incorporation of PVA facilitated the significant densification of the double-network architecture. The strong interfacial hydrogen bonding between the BC nanofibers and PVA chains fostered a synergistic interpenetrating network, ensuring efficient stress transfer and enhanced energy dissipation during deformation. Remarkably, the hydrogel maintained an exceptionally high water content of up to 95% and exhibited excellent biocompatibility, demonstrating promising potential for applications in biomedical materials.

EXPERIMENTAL

Materials

Bacterial cellulose sheets (BC) with 93% water content were purchased from Cellubio. Prior to use, the BC sheets were immersed in deionized water for 3 days to reach swelling equilibrium, resulting in a final thickness of 2 mm. Subsequently, the sheets were cut into dimensions of 3 cm × 6 cm for further use. Poly(vinyl alcohol) (M_W=1.5×10^5, 99+% hydrolyzed, Sigma-Aldrich) was purchased and directly utilized without additional purification steps. Deionized water was used as the solvent.

Preparation of BC/PVA Hydrogels

Initially, PVA solid particles and deionized water were added to blue-capped reagent bottles, which were tightly sealed to prevent water evaporation during heating. The mixtures were then stirred in an oil bath at 110 °C for 10 h to form 2 wt%, 4 wt%, 6 wt% and 8 wt% PVA solutions. Five 3 cm × 6 cm BC sheets were immersed in 200 mL of PVA solution in a sealed blue-capped reagent bottle and heated with stirring at 110 °C for an additional 10 h to ensure that PVA diffused into the voids of BC. Subsequently, BC sheets were removed from the PVA solution. The samples were frozen at –20 °C for 12 h and then thawed at 25 °C for 10 h to physically crosslink the PVA network. The freeze-thaw cycle was repeated 1–6 times to obtain the BC/PVA cryogels. The BC/PVA hydrogel was obtained by immersing the cryogels in deionized water for full swelling.

The information of "Characterizations" is detailed in the electronic supplementary information (ESI).

RESULTS AND DISCUSSION

Fabrication and Structure of BC/PVA Hydrogels

Fig. 1(a) depicts the strategy for fabricating a homogeneous

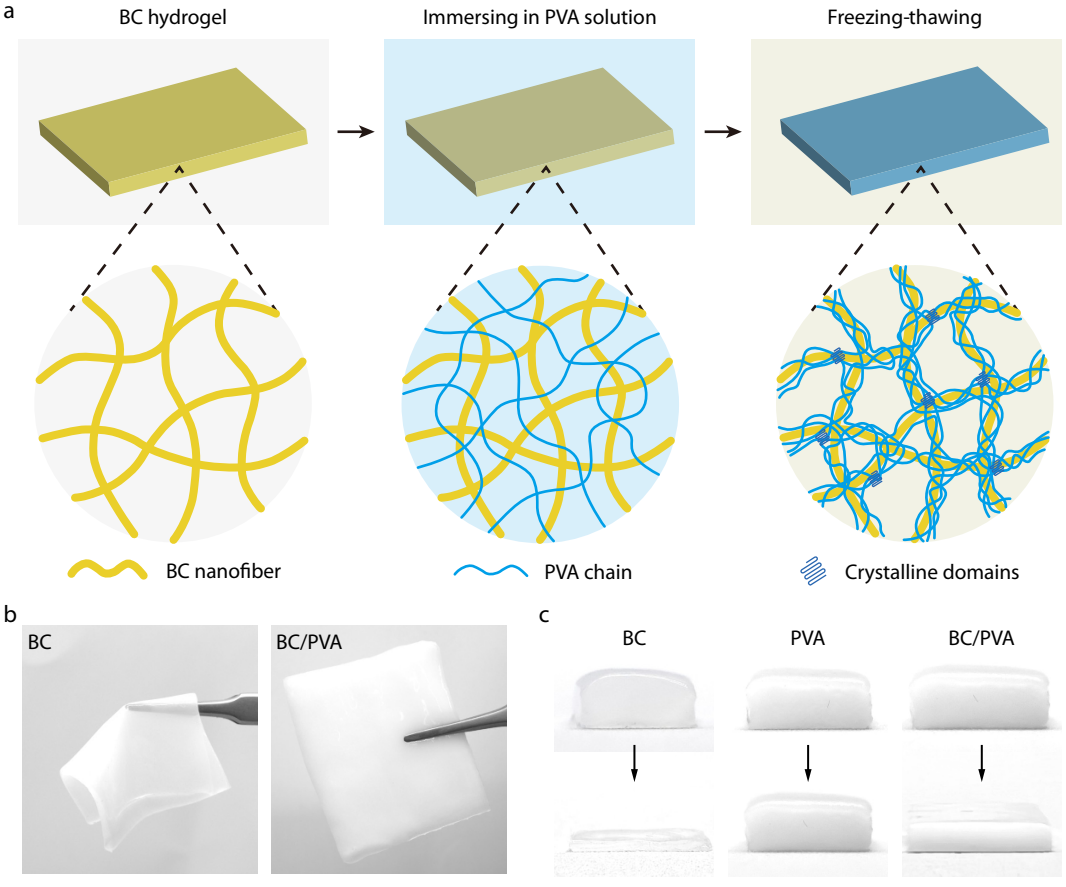

Fig. 1 (a) Schematic illustration of the fabrication of BC/PVA hydrogel; (b) Optical images of BC and BC/PVA hydrogels; (c) Optical images of hydrogels before and after 1 min compression.

double-network BC/PVA hydrogel. First, the commercial BC sheet was immersed in deionized water for three days until fully swollen, resulting in a three-dimensional network structure. The nanocellulose network was soft, and the water content was >99%. Then, the BC hydrogel was soaked in a PVA solution and heated at 110 °C under continuous stirring to accelerate PVA polymer chain mobility. Owing to the water solubility of PVA chains, PVA can diffuse into the nanocellulose network and be evenly distributed throughout the network.[41] Subsequently, the as-prepared composite was subjected to multiple freeze-thaw cycles, involving freezing at –20 °C for 12 h followed by thawing at 25 °C for 10 h. The freeze-thaw treatment induced the aggregation and crystallization of PVA chains by forming hydrogen bonds at the surface of the BC nanofibers. The abundant surface hydroxyl groups on the BC nanofibers promoted the ordered assembly of the PVA chains.[42] Repetitive freeze-thaw cycles contributed to the construction of a more compact PVA network.[41] Finally, the sample was immersed in deionized water to achieve equilibrium swelling and obtain the BC/PVA hydrogel. The BC/PVA hydrogel maintained its shape with excellent dimensional stability, whereas the BC hydrogel was soft, failing to preserve its structural integrity (Fig. 1b). When pressed in the perpendicular direction of the BC hydrogel, water was easily squeezed out from the hydrogel and failed to recover to its initial state. The PVA hydrogel was elastic and could recover its original shape. Owing to the integration of PVA, the BC/PVA hydrogel exhibited a pronounced tolerance to external compressive loads and retained partial hydration (Fig. 1c).

Mechanical Properties of BC/PVA Hydrogels

The mechanical properties of poly(vinyl alcohol)-based hydrogels are governed by the crystallinity of PVA, which is determined by both the PVA concentration and the number of freeze-thaw cycles.[43] To systematically determine the optimal PVA concentration and number of freeze-thaw cycles, tensile tests were performed on a series of BC/PVA hydrogels prepared under different conditions (Figs. 2a–2d). The tensile strain, strength, toughness, and modulus data are collectively summarized in heatmaps for a convenient comparative analysis (Figs. 2e–2h). The tensile strength of the BC/PVA hydrogels increased with the number of freeze-thaw cycles up to five cycles and remained essentially unchanged upon further increasing the number of freeze-thaw cycles. The modulus exhibits a continuous increase with increasing number of freeze-thaw cycles. Scanning electron microscopy (SEM) images reveal that the pore structure becomes increasingly pronounced after the second freeze-thaw cycle, indicating that repeated ice crystal extrusion results in a denser network architecture (Fig. S1 in ESI). The water content of the hydrogels progressively decreased with increasing number of freeze-thaw cycles, further corroborating this observation (Fig. 3). The XRD results indicate that the crystallinity of BC/PVA hydrogels increases with increasing number of freeze-thaw cycles (Fig. S2 in ESI). To quantitatively evaluate the influence of hydrogel crystallinity on the mechanical properties, the evolution of crystallinity, tensile modulus, and strength were integrated into a plot as functions of freeze-thaw cycles (Fig. S3 in ESI). The results revealed a synchronized evolution among the crystallinity, Young's modulus, and tensile strength. The characteristic peak at 1143 cm^{-1}, assigned to PVA crystalline domains, progressively intensified with increasing number of freeze-thaw cycles, corroborating this finding (Fig. S4 in ESI).

Based on a comprehensive analysis and comparison of all

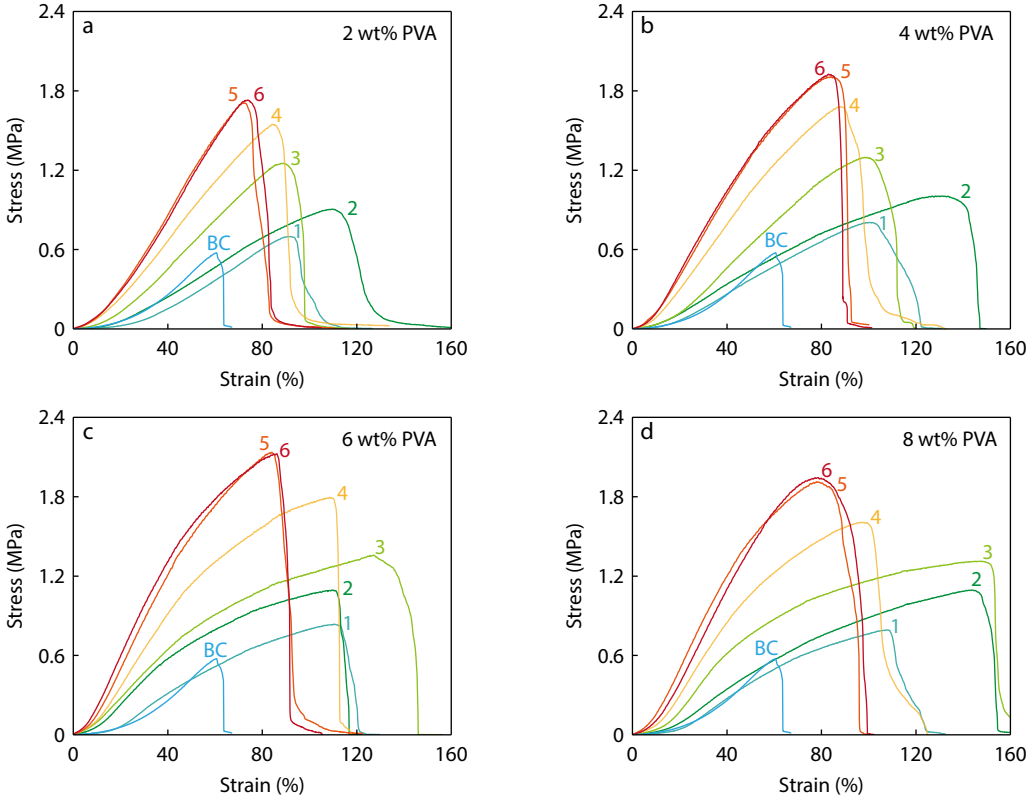

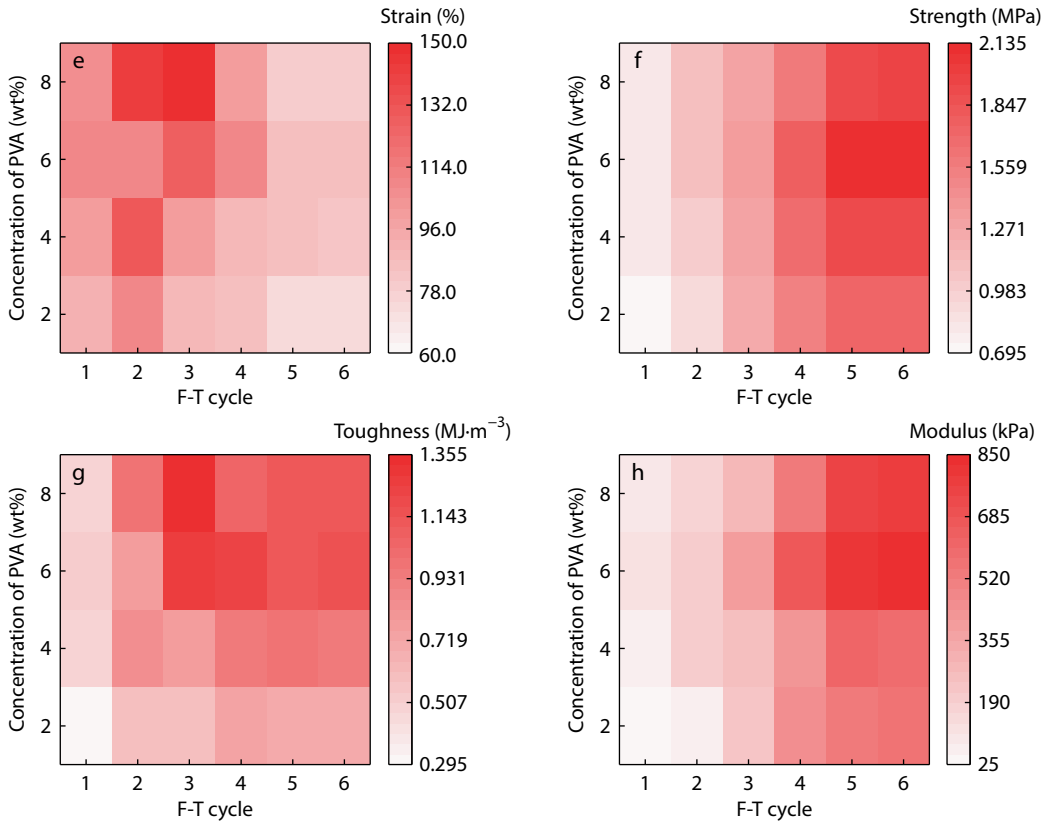

Fig. 2 Mechanical properties of BC/PVA hydrogels. (a–d) Tensile stress-strain curves of BC/PVA hydrogels prepared by freeze-thawing cycles at various concentrations of PVA solutions; (e–h) The corresponding calculated strain, strength, toughness and modulus of BC/PVA hydrogels prepared by freeze-thawing cycles at various concentrations of PVA solutions.

data, the optimal preparation parameters for the BC/PVA hydrogels were determined to be 6 wt% PVA concentration and five freeze-thaw cycles, yielding a tensile strength of (2.13±0.03) MPa, fracture strain of 84%±5%, toughness of (1.15±0.03) MJ·m^{-3}, and elastic modulus of (780±40) kPa. Unless otherwise specified, BC/PVA hydrogels were prepared under these conditions, as mentioned in the following section.

The PVA chains are inherently flexible and extensible, whereas the BC nanofibers exhibit limited stretchability owing to their densely interconnected network architecture. Therefore, the incorporation of PVA into the BC network was conducive to enhancing the mechanical properties of the resulting BC/PVA composite hydrogel. Tensile tests were conducted to study the mechanical properties of the BC, PVA, and BC/PVA hydrogels (Figs. 4a and 4b, Table S2 in ESI). The BC hydrogel exhibited a tensile strain of 60%. The PVA hydrogel demonstrated a higher fracture strain of up to 300%, whereas the tensile strength was merely 0.30 MPa. The BC/PVA hydrogels exhibited significantly enhanced mechanical properties. Compared to the pure BC hydrogel, the composite BC/PVA hydrogel exhibited a 0.4-fold increase in strain, 2.7-fold increase in strength, and 7.8-fold increase in modulus. The incorporation of PVA into the BC network compensated for the inherent lack of elasticity in BC, while simultaneously functioning as a reinforcing phase to enhance the

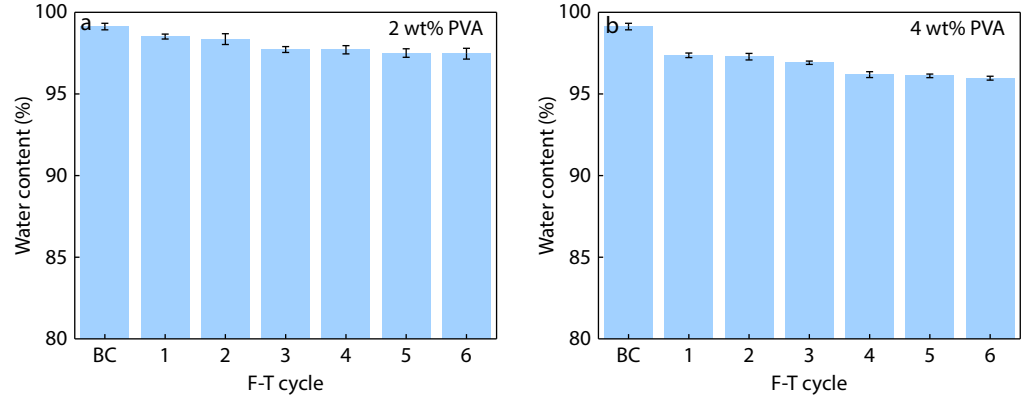

https://doi.org/10.1007/s10118-026-3684-8

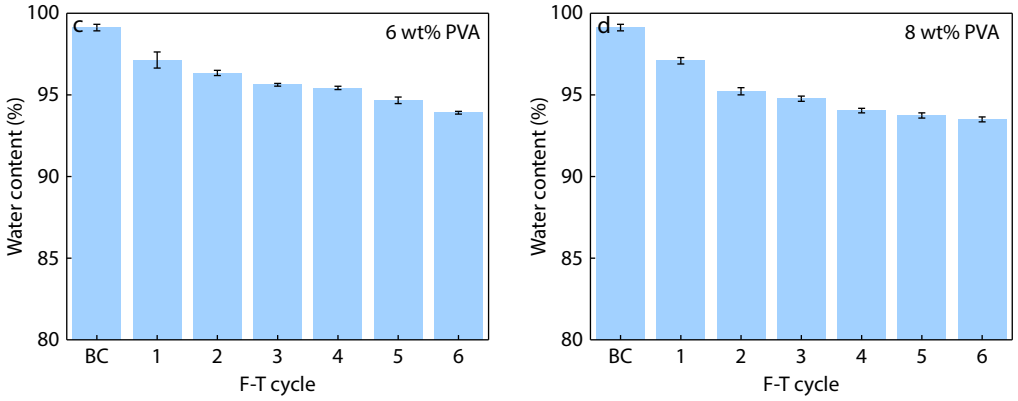

Fig. 3 Water content of BC/PVA hydrogels prepared by different concentration of PVA. (a) 2 wt% PVA, (b) 4 wt% PVA, (c) 6 wt% PVA, (d) 8 wt% PVA.

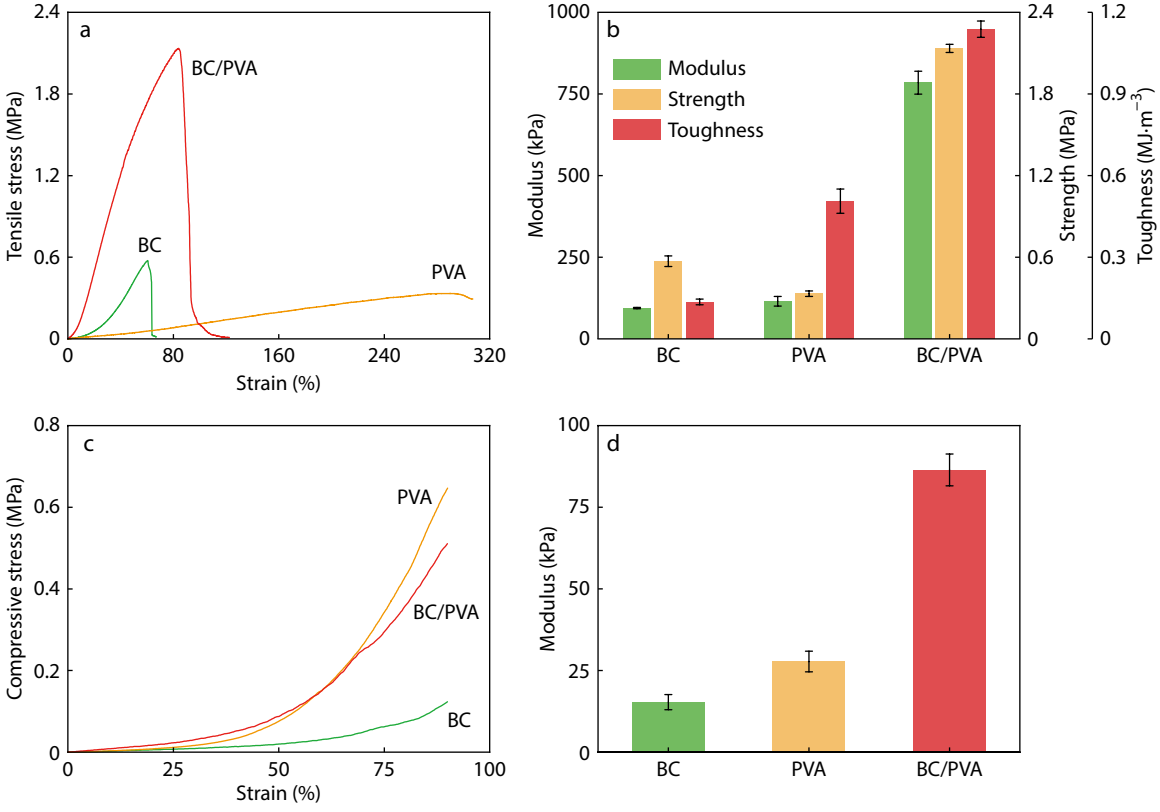

Fig. 4 Mechanical properties of hydrogels. (a) Tensile stress-strain curves and (b) tensile modulus, strength and the calculated toughness of BC, PVA and BC/PVA hydrogels; (c) Compressive stress-strain curves and (d) compressive modulus of BC, PVA and BC/PVA hydrogels. The compression strain of hydrogels was set at 90%. The error bars denote standard deviations derived from three independent measurements.

strength and modulus of the BC/PVA hydrogel.[44] The compressive tests were also conducted on the hydrogels (Figs. 4c and 4d). The results demonstrate that the BC/PVA hydrogel possesses a higher compressive modulus than the BC and PVA hydrogels. The interpenetration of PVA within the BC network also endowed the hydrogels with superior resistance to deformation.

The ability to resist crack propagation is one of the most important factors in the practical application of hydrogel materials. The BC/PVA hydrogel exhibits the highest fracture energy of (2.29±0.14) kJ·m^{-2}, which is markedly superior to that of both the BC hydrogel and the PVA hydrogel (Figs. 5a, 5b and Fig. S5, Table S2 in ESI). The presence of the PVA crystalline domains enhanced the notch resistance of the BC/PVA hydrogel.[24] Meanwhile, the energy dissipation of BC/PVA was evaluated by cyclic loading-unloading tensile tests (Figs. 5c and 5d). Under successive cyclic loading with increasing tensile strain, the energy dissipated by the hydrogel gradually increased. In addition, cyclic tensile tests were conducted on the hydrogels at a fixed strain of 10% (Figs. 5e and 5f). The results revealed that the sacrificial bonds within the hydrogel network underwent progressive rupture during repeated cycling. Nevertheless, the tensile strength remains at 0.12 MPa even after 200 loading cycles, indicating that the BC/PVA hy-

drogel maintained its ability to prevent material failure during repeated deformation.

To further elucidate the mechanical properties of the BC/PVA double-network hydrogel, rheological measurements were conducted to characterize the frequency-dependent evolution of the storage modulus (G') and loss modulus (G'') of the BC, PVA, and BC/PVA hydrogels (Fig. 6). The storage modulus exceeded the loss modulus for all hydrogels, indicating a solid-like viscoelastic behavior. Notably, the BC/PVA hydrogels exhibited a higher storage modulus than BC and PVA, suggesting that the integration of BC and PVA enhanced the density of the physical crosslinks within the BC/PVA hydrogel network. Specifically, the BC network formed a rigid scaffold through extensive hydrogen bonding and chain entanglement, while PVA chains crystallized within the BC fibrous network to serve as additional physical crosslinking sites, thereby further elevating G'. Furthermore, the BC/PVA hydrogel displays $G' > G''$, and both modulus remain distinctly separated across a broad frequency range, demonstrating the formation of interfacial interactions between the BC and PVA networks.

Mechanical Toughening Mechanism of BC/PVA Hydrogels

To reveal the underlying mechanisms governing the exceptional mechanical properties of the BC/PVA hydrogel, we compared

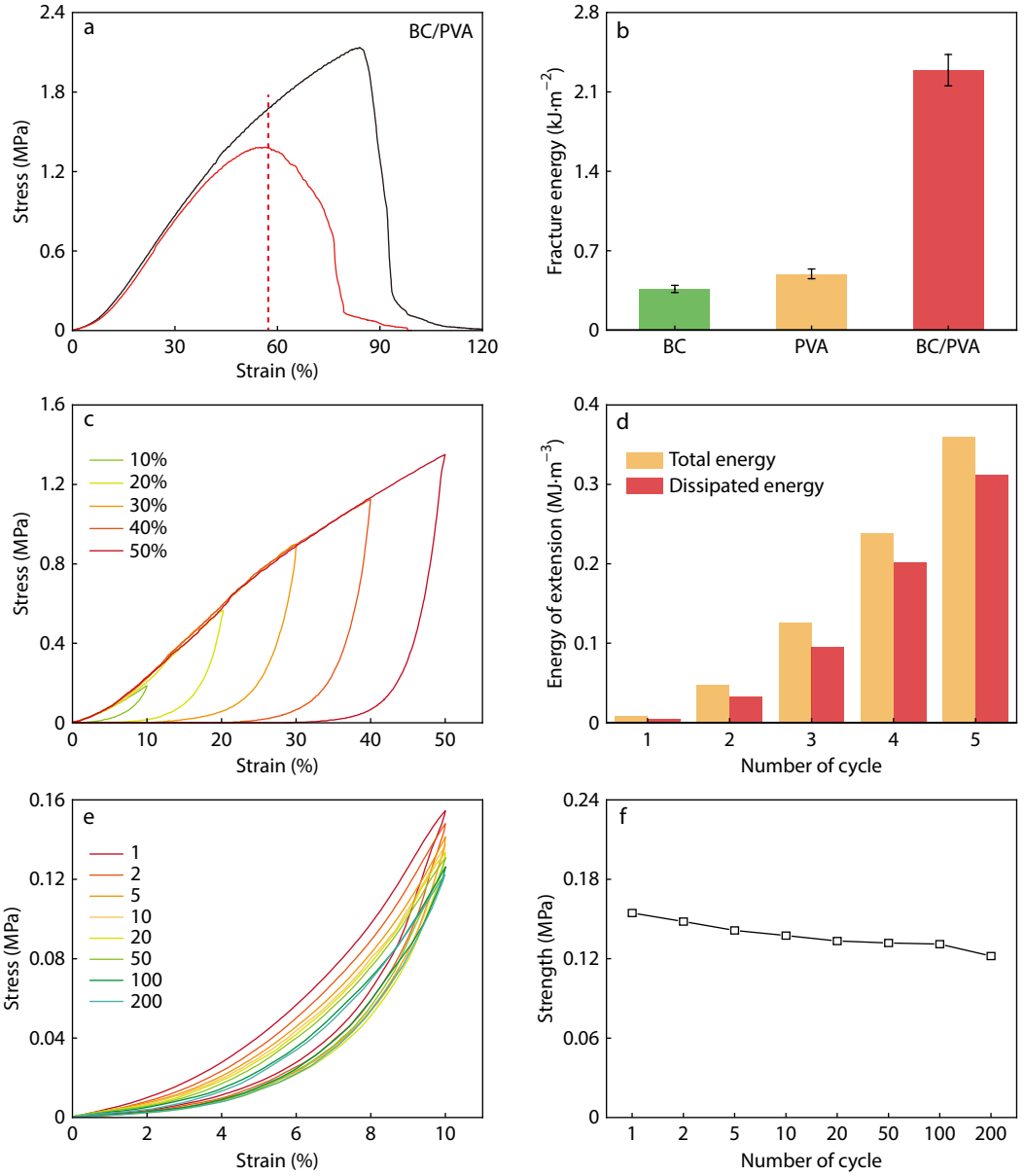

Fig. 5 Mechanical properties of hydrogels. (a) Tensile stress-strain curves of unnotched and notched BC/PVA hydrogel. The black and red lines correspond to unnotched and notched specimens, respectively. (b) The calculated fracture energy of BC, PVA and BC/PVA hydrogels. The error bars denote standard deviations derived from three independent measurements. (c) Stress-strain curves during the loading-unloading process of BC/PVA hydrogel at different strains (λ=10%–50%) and (d) total and dissipated energy. (e) Stress-strain curves during 200 cyclic loading-unloading process of BC/PVA hydrogel at 10% strain and (f) the corresponding tensile strength of different cycles.

https://doi.org/10.1007/s10118-026-3684-8

the microstructures of BC, PVA, and BC/PVA hydrogels. SEM images of the hydrogels after freeze-drying are shown in Figs. 7(a)–7(c). Clearly, BC is characterized by an ultrafine network structure, whereas PVA displays a plate-like topography. The BC/PVA hydrogel exhibited distinct porous architecture. Owing to the hydrogen bond interaction between PVA and BC, PVA encapsulates BC nanofibers and interconnects them to form an integrated network. This interconnected network architecture contributed to the enhanced mechanical performance of the hydrogels. FTIR spectroscopy was employed to characterize the evolution of intermolecular interactions within the hydrogel network (Fig. 7d). The BC/PVA hydrogel displays a characteristic peak at 1091 cm^{-1} which corresponds to the stretching vibration of C—O in PVA, confirming the successful complexation between PVA and BC. The —OH stretching peak shifted from 3305 cm^{-1} in PVA to 3324 cm^{-1} in BC/PVA, indicating the formation of hydrogen bonds between BC and PVA. The TGA results revealed that the maximum decomposition temperature of BC/PVA was higher than that of BC, indicating that the strong interfacial interaction between PVA and BC contributed to the enhanced thermal stability of the composite hydrogel (Figs. 7e and 7f).

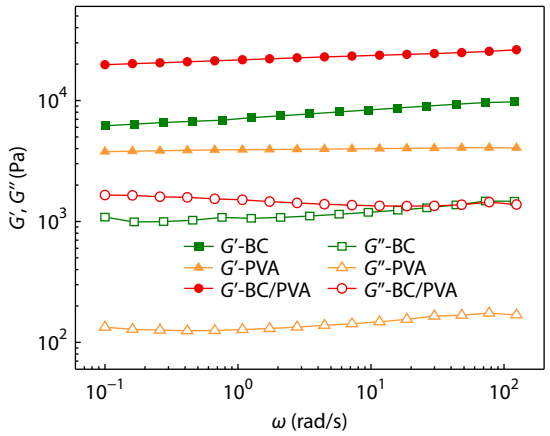

Fig. 6 The energy storage modulus *G*' and loss modulus *G*'' of BC, PVA and BC/PVA hydrogels.

To investigate microstructural evolution, wide-angle X-ray scattering (WAXS) was conducted on the BC/PVA hydrogel subjected to predetermined tensile strains. According to the WAXS results, BC displayed a diffraction peak at 22.7°, which corresponds to the typical reflection plane of (200). The peak at 19.3° arose from the (101) plane of PVA (Fig. 8a, Fig. S6 in ESI). The azimuthal angle (φ) plots of BC and PVA were characterized by two sharp peaks, indicating a highly oriented microstructure (Figs. 8b and 8c). For both BC and PVA, the orientation order parameter (*f*) exhibits a consistent trend (Fig. 8d and Fig. S7 in ESI). It increases steeply within 0%–50% strain and maintains the platform upon further deformation. Ac-

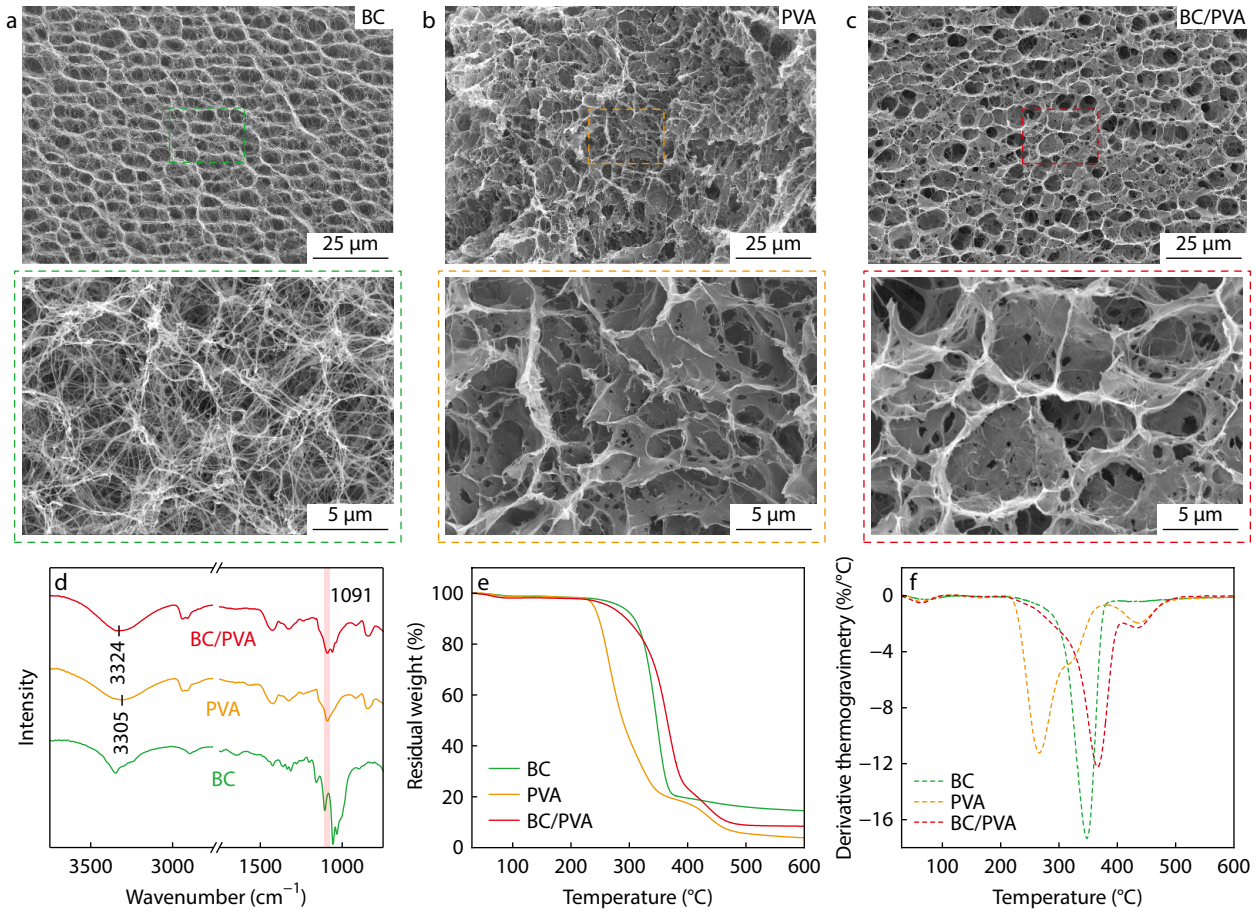

Fig. 7 Cross-sectional view of (a) BC hydrogel, (b) PVA hydrogel, and (c) BC/PVA hydrogel; (d) FTIR spectra of BC, PVA and BC/PVA; (e) Thermogravimetric and (f) derivative thermogravimetric analysis of the tested hydrogels at the heating rate of 10 °C·min^{-1}.

https://doi.org/10.1007/s10118-026-3684-8

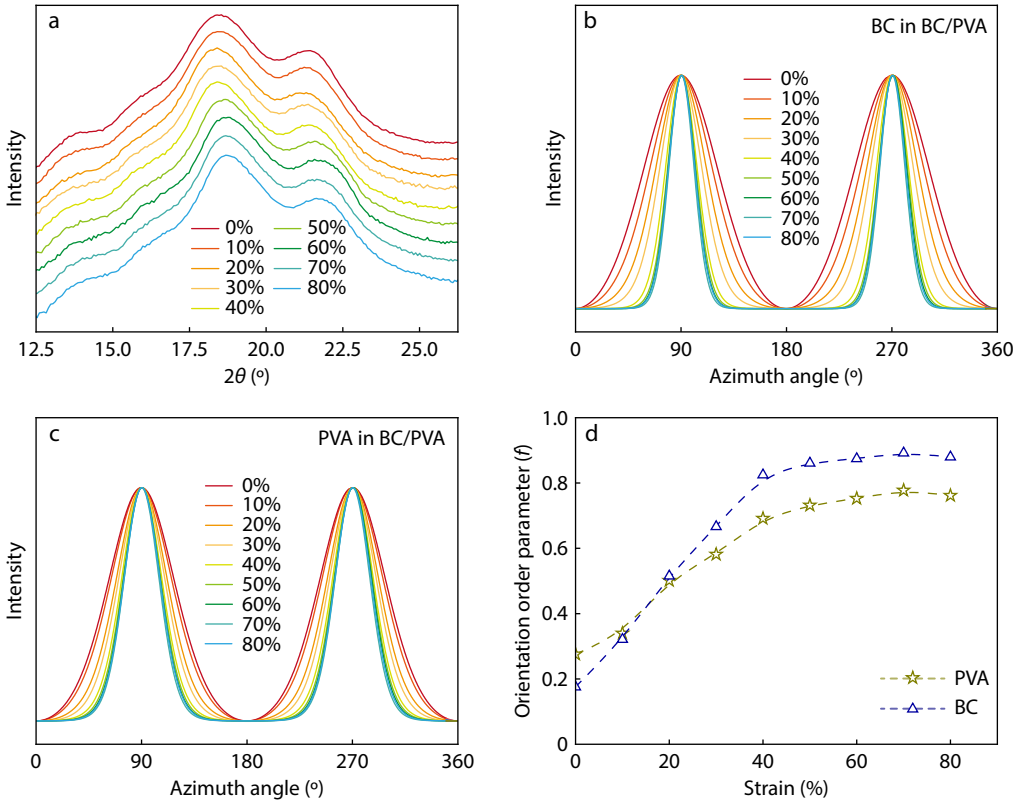

Fig. 8 (a) WAXS profiles of BC/PVA hydrogel at different stretching strains. (b, c) Plots of φ of BC and PVA of BC/PVA hydrogel at different stretching strains; (d) The orientation order parameter (f) of BC and PVA of BC/PVA hydrogel at different stretching strains.

cording to SEM and FTIR, PVA encapsulates BC nanofibers, which are coupled with abundant hydrogen bonding interactions. Hence, PVA and BC acted as integrated networks, undergoing simultaneous elongation during the tensile process. The interconnected integrated network facilitated efficient stress transfer and effective energy dissipation. Meanwhile, hydrogen bonds, regarded as sacrificial bonds, undergo rupture and reformation during the stretching process, thereby enhancing the mechanical properties of the BC/PVA hydrogel.

Biological Evaluation of BC/PVA Hydrogels

The cytotoxicity and biocompatibility of the BC/PVA hydrogel were also evaluated to explore its potential biomedical applica-

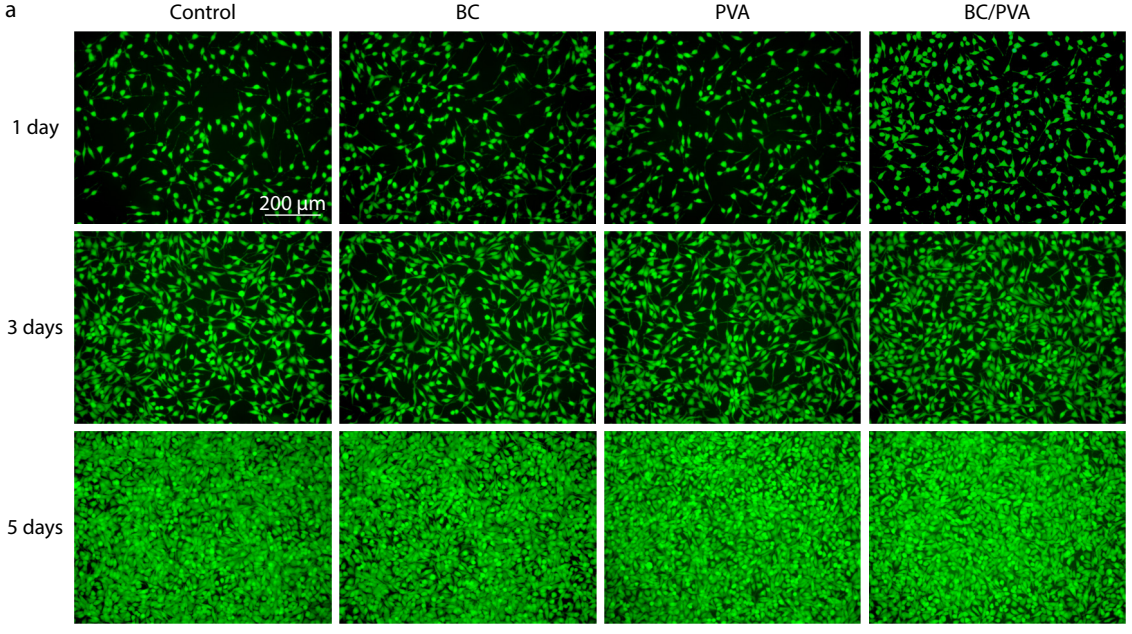

https://doi.org/10.1007/s10118-026-3684-8

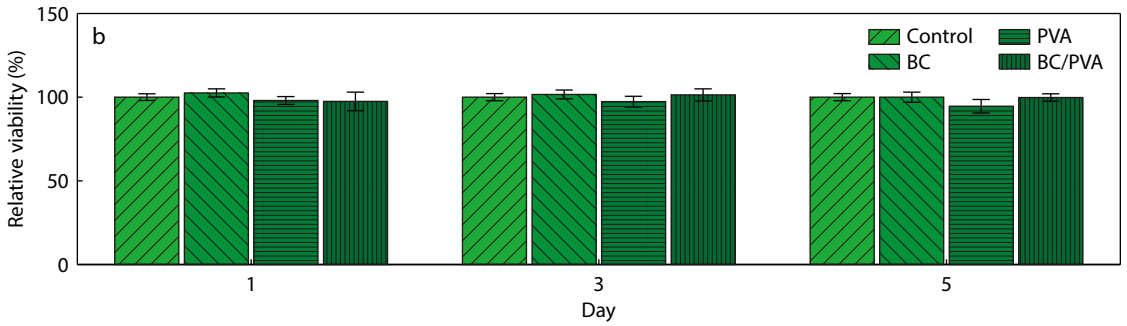

Fig. 9 Biocompatibility of BC/PVA hydrogel. (a) Fluorescence microscopy images of L-929 cells cultured with different hydrogels for different time (scale bars, 200 μm); (b) Cell viability calculated from the live/dead assay (n=3: n is the sample size for each group).

tions.[45] The cytocompatibility of the BC/PVA hydrogels was assessed following the methodology reported in a previous study. Fig. 9(a) presents the fluorescence images obtained from live/dead staining assays for BC, PVA, and BC/PVA hydrogels. Predominant green fluorescence, indicative of viable cells, was observed following incubation with the hydrogel extracts. Following exposure periods of 1, 3, and 5 days, the BC/PVA hydrogel maintained >90% cell viability (Fig. 9b). These results corroborate the outstanding biocompatibility of BC/PVA composite hydrogels, making them promising candidates for biomedical engineering applications.[46,47] Furthermore, the hydrogel maintained a superior structural integrity in diverse physiological environments (Fig. S8 in ESI), suggesting their suitability for various biomedical platforms.

CONCLUSIONS

In summary, we have developed a facile method for the fabrication of the double-network hydrogels through multiple freeze-thaw cycles. The synergistic effects of hydrogen bonding interaction and network densification collectively endow the BC/PVA hydrogel with excellent mechanical performance, for example, tensile strength of (2.13±0.03) MPa, toughness of (1.15±0.03) $MJ{\cdot}m^{-3}$, and elastic modulus of (780±40) kPa. Moreover, the hydrogel had a high water content (up to 95%). The absence of chemical crosslinking agents or additives endowed the BC/PVA hydrogel with excellent biocompatibility. This methodology represents a promising and versatile approach for the fabrication of strong and tough high-water content hydrogels tailored for biomedical applications.

Conflict of Interests

The authors declare no interest conflict.

Electronic Supplementary Information

Electronic supplementary information (ESI) is available free of charge in the online version of this article at http://doi.org/10.1007/s10118-026-3684-8.

Data Availability Statement

The data supporting the findings of this study are available from the corresponding author upon reasonable request. Author's contact information: kongsw@ustc.edu.cn and zhaochuangqi@ustc.edu.cn.

ACKNOWLEDGMENTS

This work was financially supported by the National Natural Science Foundation of China (Nos. 22305244 and 2252200918), CAS Hundred Talent Program (No. KJ2060007007), and Suzhou Key Laboratory of Bioinspired Interfacial Science (No. SZ2024004). This research was also supported by the Physical and Chemical Analysis Center of the Suzhou Institute for Advanced Research, University of Science and Technology of China.

REFERENCES

1 Zhao, X.; Chen, X.; Yuk, H.; Lin, S.; Liu, X.; Parada, G. Soft materials by design: unconventional polymer networks give extreme properties. *Chem. Rev.* **2021**, *121*, 4309–4372.
2 Zhang, Q.; Liu, Y.; Yang, G.; Kong, H.; Guo, L.; Wei, G. Recent advances in protein hydrogels: from design, structural and functional regulations to healthcare applications. *Chem. Eng. J.* **2023**, *451*, 138494.
3 Zhang, L.; Lee, W.; Li, X.; Jiang, Y.; Fang, X.; Dai, G.; Liu, Y. 3D direct printing of mechanical and biocompatible hydrogel metastructures. *Bioact. Mater.* **2022**, *10*, 48–55.
4 Liu, Z.; Zhang, H.; Zhou, R.; Gao, H.; Wu, Y.; Wang, Y.; Wu, H.; Guan, C.; Wang, L.; Tang, L.; Song, P.; Xue, H.; Gao, J. Thermoplastic elastomer-reinforced hydrogels with excellent mechanical properties, swelling resistance, and biocompatibility. *Adv. Sci.* **2025**, *12*, 2414339.
5 Xiao, W.; Wu, H.; Su, Q.; Yan, J.; Tang, L.; Huang, X.; Lu, L.; Gu, W.; Song, P.; Gao, J. MXene initiated in situ construction of superhydrophobic and electrically conductive nanofibrous composites for wearable multifunctional sensing. *Chem. Eng. J.* **2025**, *508*, 161074.
6 Peng, R.; Ba, F.; Li, J.; Cao, J.; Zhang, R.; Liu, W.-Q.; Ren, J.; Liu, Y.; Li, J.; Ling, S. Embedding living cells with a mechanically reinforced and functionally programmable hydrogel fiber platform. *Adv. Mater.* **2023**, *35*, 2305583.
7 Zhou, D.; Wang, W.; Ma, W.; Xian, Y.; Zhang, Z.; Pan, Z.; Li, Y.; Huang, L.; Liu, L.; Zheng, Z.; Liu, H.; Wu, D. Cartilage-adaptive hydrogels *via* the synergy strategy of protein templating and mechanical training. *Adv. Mater.* **2025**, *37*, 2414081.
8 Asim, S.; Tuftee, C.; Qureshi, A. T.; Callaghan, R.; Geary, M. L.; Santra, M.; Pal, V.; Namli, I.; Yam, G.; Ozbolat, I. T.; Rizwan, M.

Graphical Abstract

Strong and Tough High-water Content Double-network Hydrogels

Shu-Xing Yin, Guo-Jun Che, Cheng Qian, Meng Yu, Can Zhou, Sheng-Wen Kong, Chuang-Qi Zhao, and Lei Jiang

University of Science and Technology of China

This study proposes a strategy to fabricate strong and tough double-network hydrogels through multiple freeze-thaw cycles. Network densification endows hydrogels with exceptional mechanical performance. Moreover, the hydrogel possessed a high water content (up to 95%) and excellent biocompatibility.

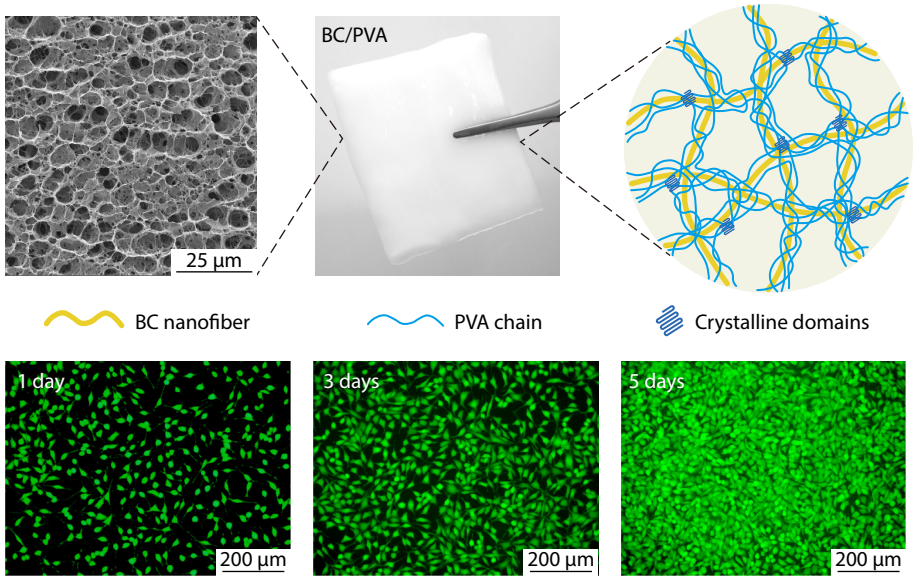

Chinese J. Polym. Sci. 2026, 44, 1738–1748 *https://doi.org/10.1007/s10118-026-3684-8*

Multi-functional gelatin-dithiolane hydrogels for tissue engineering. *Adv. Funct. Mater.* **2025**, *35*, 2407522.

9 López-Díaz, A.; Vázquez, A. S.; Vázquez, E. Hydrogels in soft robotics: past, present, and future. *ACS Nano* **2024**, *18*, 20817–20826.

10 Nasseri, R.; Bouzari, N.; Huang, J.; Golzar, H.; Jankhani, S.; Tang, X.; Mekonnen, T.-H.; Aghakhani, A.; Shahsavan, H. Programmable nanocomposites of cellulose nanocrystals and zwitterionic hydrogels for soft robotics. *Nat. Commun.* **2023**, *14*, 6108.

11 Fu, D.; Xing, L.; Xie, Y.; Li, P.; Yang, F.; Sui, X.; Liu, J.; Chi, J.; Huang, B.; Shen, J. Hybrid crosslinking cellulose nanofibers-reinforced zwitterionic poly (ionic liquid) organohydrogel with high-stretchable, anti-freezing, anti-drying as strain sensor application. *Carbohyd. Polym.* **2025**, *353*, 123253.

12 Gong, X.; Luo, Y.; Zhang, C.; Xie, J.; Wang, Y. Carboxymethyl chitosan-based tough hydrogels with low mechanical hysteresis and high conductivity as multifunctional sensors. *Chem. Eng. J.* **2025**, *510*, 161610.

13 Han, F.; Chen, S.; Wang, F.; Liu, M.; Li, J.; Liu, H.; Yang, Y.; Zhang, H.; Liu, D.; He, R.; Cao, W.; Qin, X.; Xu, F. High-conductivity, self-healing, and adhesive ionic hydrogels for health monitoring and human-machine interactions under extreme cold conditions. *Adv. Sci.* **2025**, *12*, 2412726.

14 Liu, H.; Guan, S.; Wang, P.; Dong, X. Super tough anti-freezing and antibacterial hydrogel with multi-crosslinked network for flexible strain sensor. *Small* **2025**, *21*, 2407870.

15 Liu, S.; Zhan, H.; Wu, P.; Lei, Z. Underwater-stable conductive hydrogels: From molecular design to next-generation aquatic sensors. *Chin. J. Chem.* **2026**, *44*, 571–582.

16 Xia, P.; Zhang, W.; Peng, C.; Yin, H.; Wang, D.; Yang, J.; Tuan, R.-S.; Jiang, L.; Wang, J. A high-order double network hydrogel. *Macromolecules* **2024**, *57*, 11251–11265.

17 Fang, Y.; Liang, C.; Liljestrom, V.; Lv, Z.; Ikkala, O.; Zhang, H. Toughening hydrogels with fibrillar connected double networks. *Adv. Mater.* **2024**, 2402282.

18 Surhadi, J. U.; Aymon, B.; Carton, M.; Porerla, C. M. Double-network-inspired mechanical metamaterials. *Nat. Mater.* **2025**, *24*, 945–954.

19 Gu, Y.; Wu, W.; Zhang, C.; Li, X.; Guo, X.; Wang, Y.; Yuan, Y.; Jiang, B.; Jin, Y. Multi-solvent-induced gradient aggregation rendered superstrong, tough, stretchable, and fatigue-resistant lignin-based supramolecular hydrogels. *Adv. Funct. Mater.* **2025**, *35*, 2417206.

20 Hong, S.; Lee, J.; Park, T.; Jeong, J.; Lee, J.; Joo, H.; Mesa, J.; Alston, C.-B.; Ji, Y.; Vega, S. R.; Barinaga, C.; Yi, J.; Lee, Y.; Kim, J.; Won, K.; Solorio, L.; Kim, Y.; Lee, H.; Kim, D. R.; Lee, C. H. Spider silk-inspired conductive hydrogels for enhanced toughness and environmental resilience *via* dense hierarchical structuring. *Adv.*

Sci. **2025**, *12*, 2500397.
21 Wu, S.; Liu, Z.; Gong, C.; Li, W.; Xu, S.; Wen, R.; Feng, W.; Qiu, Z.; Yan, Y. Spider-silk-inspired strong and tough hydrogel fibers with anti-freezing and water retention properties. *Nat. Commun.* **2024**, *15*, 4441.
22 Jiang, Y.; Tang, N.; Wang, X.; Pei, D.; Zhang, H.; Li, M.; Hu, J. Mechanically robust eutectogels enabled by precisely engineered crystalline domains. *Nat. Commun.* **2025**, *16*, 7417.
23 Tang, N.; Jiang, Y.; Wei, K.; Zheng, Z.; Zhang, H.; Hu, J. Evolutionary reinforcement of polymer networks: a stepwise-enhanced strategy for ultra-robust eutectogels. *Adv. Mater.* **2023**, *36*, 2309576.
24 Zhu, S.; Wang, S.; Huang, Y.; Tang, Q.; Fu, T.; Su, R.; Fan, C.; Xia, S.; Lee, P.-S.; Lin, Y. Bioinspired structural hydrogels with highly ordered hierarchical orientations by flow-induced alignment of nanofibrils. *Nat. Commun.* **2024**, *5*, 118.
25 Xu, L.; Qiao, Y.; Qiu, D. Coordinatively stiffen and toughen hydrogels with adaptable crystal-domain cross-linking. *Adv. Mater.* **2023**, *35*, 2209913.
26 Wu, Y.; Zhang, Y.; Wu, H.; Wen, J.; Zhang, S.; Xing, W.; Zhang, H.; Xue, H.; Gao, J.; Mai, Y. Solvent-exchange-assisted wet annealing: a new strategy for superstrong, tough, stretchable, and anti-fatigue hydrogels. *Adv. Mater.* **2023**, *35*, 2210624.
27 Zhang, Y.; Liu, L.; Yin, S.; Zhou, C.; Ding, Y.; Che, G.; Zhao, C. Underwater high strength and tough polyvinyl alcohol-polyacrylic acid hydrogel. *Adv. Funct. Mater.* **2025**, 2503023.
28 Bao, B.; Zeng, Q.; Li, K.; Wen, J.; Zhang, Y.; Zheng, Y.; Zhou, R.; Shi, C.; Chen, T.; Xiao, C.; Chen, B.; Wang, T.; Yu, K.; Sun, Y.; Lin, Q.; He, Y.; Tu, S.; Zhu, L. Rapid fabrication of physically robust hydrogels. *Nat. Mater.* **2023**, *22*, 1253.
29 Wang, S.; Yu, Z.; Sun, X.; Panahi-Sarmad, M.; Yang, P.; Zhu, P.; Zhu, Y.; Liu, H.; Jiang, F. A universal strategy to mitigate microphase separation *via* cellulose nanocrystal hydration in fabricating strong, tough, and fatigue-resistant hydrogels. *Adv. Mater.* **2024**, 2416916.
30 Kim, J.; Zhang, G.; Shi, M.; Suo, Z. Fracture, fatigue, and friction of polymers in which entanglements greatly outnumber cross-links. *Science* **2021**, *374*, 212–216.
31 Zhu, R.; Zhu, D.; Zheng, Z.; Wang, X. Tough double network hydrogels with rapid self-reinforcement and low hysteresis based on highly entangled networks. *Nat. Commun.* **2024**, *15*, 1344.
32 Liang, C.; Dudko, V.; Khoruzhenko, O.; Hong, X.; Lv, Z.; Tunn, I.; Umer, M.; Timonen, J.; Linder, M.-B.; Breu, J.; Ikkala, O.; Zhang, H. Stiff and self-healing hydrogels by polymer entanglements in co-planar nanoconfinement. *Nat. Mater.* **2025**, *24*, 599–606.
33 Zhang, H.; Chen, L.; Xiao, Y.; Guo, X.; Zhao, S.; Guan, R.; Long, T.; Cheng, X.; Zhou, C. Development of strong and tough silicone hydrogels enabled by polymerization-induced microphase separation and multiscaled electrostatic interactions and their application as water-shrinkable sleeves. *Adv. Funct. Mater.* **2025**, e07061.
34 Huo, H.; Shen, J.; Wan, J.; Shi, H.; Yang, H.; Duan, X.; Gao, Y.; Chen, Y.; Kuang, F.; Li, H.; Yang, L.; Du, G. A tough and robust hydrogel constructed through carbon dots induced crystallization domains integrated orientation regulation. *Nat. Commun.* **2025**, *16*, 6221.
35 Fu, L.; Li, L.; Bian, Q.; Xue, B.; Jin, J.; Li, J.; Cao, Y.; Jiang, Q.; Li, H. Cartilage-like protein hydrogels engineered *via* entanglement. *Nature* **2023**, *618*, 740.
36 Picheth, G. F.; Pirich, C. L.; Sierakowski, M. R.; Woehl, M. A.; Sakakibara, C. N.; de Souza, C. F.; Martin, A.-A.; da Silva, R.; de Freitas, R. A. Bacterial cellulose in biomedical applications: A review. *Int. J. Biol. Macromol.* **2017**, *104*, 97–106.
37 Li, X.; Yuan, L.; Liu, R.; He, H.; Hao, J.; Lu, Y.; Wang, Y.; Liang, G.; Yuan, G.; Guo, Z. Engineering textile electrode and bacterial cellulose nanofiber reinforced hydrogel electrolyte to enable high-performance flexible all-solid-state supercapacitors. *Adv. Energy Mater.* **2021**, *11*, 2003010.
38 Nakayama, A.; Kakugo, A.; Gong, J.-P.; Osada, Y.; Takai, M.; Erata, T.; Kawano, S. High mechanical strength double-network hydrogel with bacterial cellulose. *Adv. Funct. Mater.* **2004**, *14*, 1124–1128.
39 Guan, Q.; Han, Z.; Zhu, Y.; Xu, W.; Yang, H.; Ling, Z.; Yan, B.; Yang, K.; Yin, C.; Wu, H.; Wu, H. Bio-inspired lotus-fiber-like spiral hydrogel bacterial cellulose fibers. *Nano Lett.* **2021**, *21*, 952–958.
40 Park, D.; Kim, J. W.; Shin, K.; Kim, J.-W. Bacterial cellulose nanofibrils-reinforced composite hydrogels for mechanical compression-responsive on-demand drug release. *Carbohyd. Polym.* **2021**, *272*, 118459.
41 Kim, J.; Choi, J.; Hyun, J. Free-form three-dimensional nanocellulose structure reinforced with poly(vinyl alcohol) using freeze-thaw process. *Carbohyd. Polym.* **2022**, *298*, 120055.
42 Liu, D.; Sun, X.; Tian, H.; Maiti, S.; Ma, Z. Effects of cellulose nanofibrils on the structure and properties on PVA nanocomposites. *Cellulose* **2013**, *20*, 2981–2989.
43 Soto-Bustamante, F.; Bassu, G.; Fratini, E.; Laurati, M. Effect of composition and freeze-thaw on the network structure, porosity and mechanical properties of polyvinyl-alcohol/chitosan hydrogels. *Gels* **2023**, *9*, 396.
44 Wan, W.; Bannerman, A. D.; Yang, L.; Mak, H., in *Polymeric cryogels*, Springer, Switzerland, **2014**, p. 283.
45 Zhu, T.; Ni, Y.; Biesold, G. M.; Cheng, Y.; Ge, M.; Li, H.; Huang, J.; Lin, Z.; Lai, Y. Recent advances in conductive hydrogels: classifications, properties, and applications. *Chem. Soc. Rev.* **2023**, *52*, 473–509.
46 Eivazzadeh-Keihan, R.; Noruzi, E. B.; Aliabadi, H. A. M.; Sheikhaleslami, S.; Akbarzadeh, A. R.; Hashemi, S. M.; Gorab, M. G.; Maleki, A.; Cohan, R. A.; Mahdavi, M.; Poodat, R.; Keyvanlou, F.; Esmaeili, M. S. Recent advances on biomedical applications of pectin-containing biomaterials. *Int. J. Biol. Macromol.* **2022**, *217*, 1–18.
47 Li, X.; Zhang, L.; Liu, Z.; Wang, R.; Jiao, T. Recent progress in hydrogels combined with phototherapy for bacterial infection: a review. *Int. J. Biol. Macromol.* **2024**, *274*, 133375.